

Accepted Article

Title: Vertical Graphene Arrays with Straightaway Ions Capacitance for AC Line-Filtering Capacitors

Authors: Shichen Xu, Yeye Wen, Zhuo Chen, Nannan Ji, Zhigang Zou, Mingmao Wu, Liangti Qu, and Jin Zhang

This manuscript has been accepted after peer review and appears as an Accepted Article online prior to editing, proofing, and formal publication of the final Version of Record (VoR). This work is currently citable by using the Digital Object Identifier (DOI) given below. The VoR will be published online in Early View as soon as possible and may be different to this Accepted Article as a result of editing. Readers should obtain the VoR from the journal website shown below when it is published to ensure accuracy of information. The authors are responsible for the content of this Accepted Article.

To be cited as: *Angew. Chem. Int. Ed.* 10.1002/anie.202111468

Link to VoR: <https://doi.org/10.1002/anie.202111468>

COMMUNICATION

Vertical Graphene Arrays with Straightaway Ions Capacitance for AC Line-Filtering Capacitors

Shichen Xu,^[a,c] Yeye Wen,^[a,c] Zhuo Chen,^[a,c] Nannan Ji,^[c] Zhigang Zou,^[b,f] Mingmao Wu,^{*[b]} Liangti Qu,^{*[e]} Jin Zhang^{*[a,c,d]}

- [a] S. C. Xu, Dr. Y. Y. Wen, Dr. Z. Chen, Prof. J. Zhang
Center for Nanochemistry, Beijing Science and Engineering Center for Nanocarbons, Beijing National Laboratory for Molecular Sciences, College of Chemistry and Molecular Engineering, Peking University
Beijing 100871, P. R. China
E-mail: jinzhang@pku.edu.cn
- [b] Prof. Z. G. Zou, Prof. M. M. Wu
Key Laboratory of Eco-materials Advanced Technology, College of Materials Science and Engineering, Fuzhou University
Fuzhou 350108, P. R. China
E-mail: wumm20@fzu.edu.cn
- [c] S. C. Xu, Dr. Y. Y. Wen, Dr. Z. Chen, N. N. Ji, Prof. J. Zhang
Beijing Graphene Institute (BGI)
Beijing, 100095, P. R. China
- [d] Prof. J. Zhang
School of Materials Science and Engineering, Peking University
Beijing, 100095, P. R. China
- [e] Prof. L. T. Qu
Department of Chemistry, Tsinghua University
Beijing 100871, P. R. China
E-mail: lqu@tsinghua.edu.cn
- [f] Prof. Z. G. Zou
National Laboratory of Solid State Microstructures, Department of Physics, Nanjing University
Nanjing 210093, P. R. China

Abstract: High-frequency responsive electrochemical capacitor (EC), as an ideal lightweight filtering capacitor, can directly convert alternating current (AC) to direct current (DC). However, current electrodes are stuck in limited electrode area and tortuous ion transport. Herein, strictly vertical graphene arrays (SVGAs) prepared by electric-field-assisted plasma enhanced chemical vapour deposition have been successfully designed as the main electrode to ensure ions rapidly adsorb/desorb in richly available graphene surface. SVGAs exhibit an outstanding specific areal capacitance of $1.72 \text{ mF}\cdot\text{cm}^{-2}$ at $\Phi_{120} = 80.6^\circ$ even after 500,000 cycles, which is far better than that of most carbon-related materials. Impressively, the output voltage could also be improved to 2.5 V when using organic electrolyte. An ultra-high energy density of $0.33 \text{ }\mu\text{Wh}\cdot\text{cm}^{-2}$ can also be handily achieved. Moreover, ECs-SVGAs can well smooth arbitrary AC waveforms into DC signals, exhibiting excellent filtering performance.

With the rapid development of electronic products toward lightweight and miniaturization, electrochemical capacitors (ECs) with fast rate capability, appreciable capacitance density, and appropriate flexibility have attracted extensive attention.¹⁻⁶ In particular, the high-frequency responsive EC, which smooth the leftover alternate currents (AC) ripples into direct currents (DC) in line-powered devices, is an encouraging alternate for the bulky and rigid aluminum electrolytic capacitor (AEC).⁷⁻¹⁴ However, integration of high energy density and high frequency response properties within a tiny EC device still remains a challenge, which lies in mutually exclusive requirements for complex electrode structures.¹⁵⁻²¹

Given this, a myriad of electrode materials with elaborate structures have been developed to balance the trade-offs between the ion transport property and capacitance density,

including the vertically aligned arrays, large porous films, onion-like nanoparticles, edge-oriented coating, coordination polymer framework, and their composite assemblies.²²⁻⁴¹ Among them, vertical graphene (VG) holding straightly open channels and abundant charge storage surfaces are ideal electrodes for excellent AC line filtering.

However, using most popular electrochemical deposition method, a quasi-vertical structure can be fabricated with graphene oxide or reduced graphene oxide, which leads to limited accessible electrode surface areas and heavily intensified electrolyte resistance.^{7, 10} Instead, plasma-enhanced chemical vapor deposition (PECVD) can directly grow a conductive VG with strictly vertical channels on collectors in one step, which allows the ions to quickly reach the whole pores. Unfortunately, the reported VG electrodes prepared by traditional PECVD exhibit limited electrode height ($\sim 2 \text{ }\mu\text{m}$)^{25, 42, 43} and randomly arranged graphene sheets, impeding the maximum capacitance.⁴⁴⁻⁴⁹ Therefore, it is highly desirable to simultaneously enhance growth rate and accurately controlling the orientation of VG for high performance electrode materials.

Herein, we developed an electric-field assisted plasma-enhanced chemical vapor deposition (EF-PECVD) method to grow strictly vertical graphene arrays (SVGAs) as electrode materials of ECs. Benefiting from in-built electric field, graphene arrays could grow vertically and bond to each other at a height of $\sim 30 \text{ }\mu\text{m}$, forming a conductive network in the horizontal direction and micro-channel in the vertical direction. Moreover, free-standing graphene sheets and the connection between directly grown graphene endow the capacitors with high SSA and smooth ion channels. Hence, SVGAs exhibit an excellent specific areal capacitance (C_A) of 1.72

COMMUNICATION

mF cm^{-2} at $\Phi_{120} = 80.6^\circ$ in aqueous ECs, which is over 19 times higher than that of graphene sheets grown with traditional PECVD and better than that of all the quasi-vertical electrodes. Moreover, the output voltage could also be improved to 2.5 V by using the organic electrolyte. Accordingly, an ultra-high energy density of $0.33 \mu\text{Wh}\cdot\text{cm}^{-2}$ at $\Phi_{120} = 80.1^\circ$ can be achieved. Furthermore, both aqueous and organic SVGAs-ECs can well smooth arbitrary AC waveforms into DC signals, demonstrating outstanding filtering functions in diversified scenarios.

Construction of SVGAs and ECs

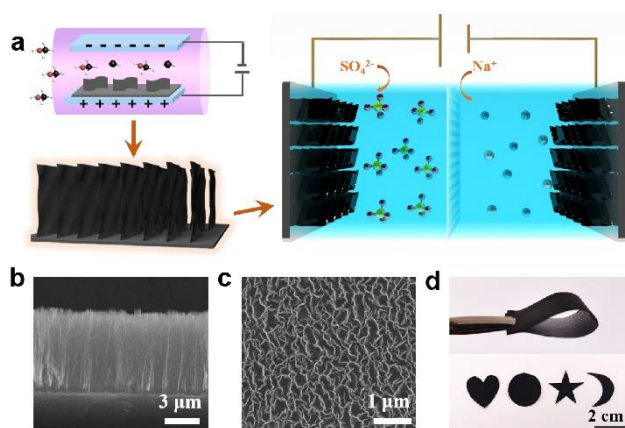


Figure 1. Synthetic procedure and morphology characterization of electrode materials for EC. **a** Schematic illustrations of EF-PECVD procedure for growth of SVGAs and construction of SVGAs based EC. **b**, **c** sectional-view and top-view SEM images of SVGAs. **d** digital photo of SVGAs electrode with flexibility and machinability.

Figure 1a illustrates the overall synthetic procedure for the growth of SVGAs and preparation of flexible ECs constructed by SVGAs. SVGAs are prepared by a homemade EF-PECVD setup equipped with two parallel electrode pads (upper-left in **Figure 1a** and **Figure S1**) which induce a constant vertical electric field.⁵⁰ During the growth procedure, the reactive carbon species generated from plasma bombardment can continuously converge and nucleate on the substrate, then piece together into graphene sheets. The built-in electric field induce a dipole moment (P) on graphene. Later, a force (F_R) produced on the dipole would continuously rotate VG sheets and align them along with the electric field orientation (**Figure S2**), thus forming a strict 90° graphene wall on the substrates (lower-left in **Figure 1a**).⁵¹ Typical side-view scanning electronic microscope (SEM) images (**Figure 1b**) represents a free-standing structure, in which all graphene sheets stand vertically on substrates without any tortuosity. Impressively, the electric field could maintain the vertical structure of SVGAs up to $30 \mu\text{m}$ or even higher (**Figure S3**), which is of good crystalline quality and has no metal and other impurities (**Figure S4**). Moreover, in top-view SEM image, SVGAs exhibit small pore sizes ($\sim 500 \text{ nm}$) with abundant active edges and non-agglomerated morphology (**Figure 1c**). Besides, the growth of SVGAs is a low temperature, catalyst-free, and universal procedure, making it possible to grow a large area SVGAs electrode on various substrates with flexibility and arbitrary shapes (**Figure 1d** and **Figure S5**). Finally, the ECs with

sandwich configuration are prepared by face to face placing two identical electrodes and exhibit a compact and portable appearance (the right column of **Figure 1a** and **Figure S6**), delivering good compatibility with miniaturized electronic circuits.

Comparison between SVGAs and QVGAs

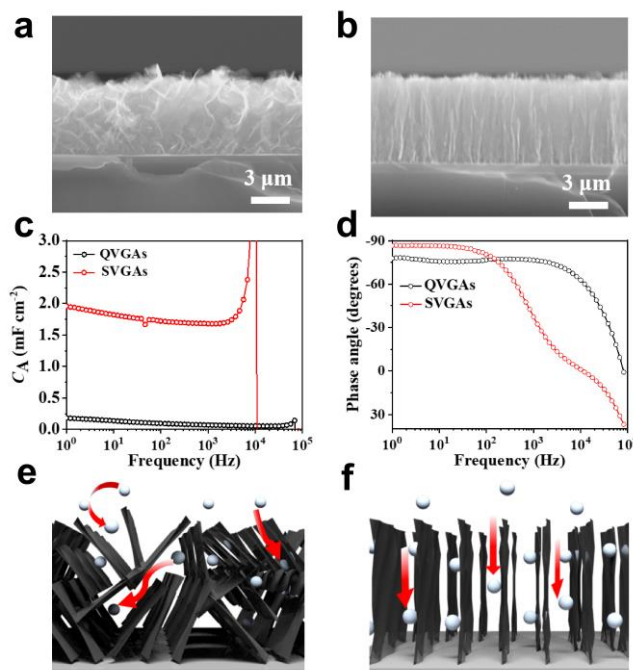


Figure 2. Comparison of structural and electrochemical properties between QVGAs and SVGAs. **a**, **b** Sectional-view SEM images of QVGAs and SVGAs. **c**, **d** Plots of phase angle and areal specific capacitance (C_A) versus frequency for EC-SVGAs and EC-QVGAs, respectively. **e**, **f** Schematic illustration of ion diffusion in QVGAs and SVGAs, respectively.

Figure 2a and **2b** display the cross-sectional microscope images of two different vertical electrode materials grown by PECVD without and with an additional electric field. As the growth time increases, the graphene sheets of QVGAs will overlap and splice with each other and eventually form a dense three-dimensional nanowall structure, (**Figure 2a**) in sharp contrast to the 90° vertical SVGAs. (**Figure 2b**) Their morphological characteristics are also verified by the transmission electron microscopy (TEM) (**Figure S7**).

Furthermore, to directly reveal the superiority of SVGAs over QVGAs, the EC based on SVGAs (EC-SVGAs) and QVGAs (EC-QVGAs) with the same height of $\sim 6 \mu\text{m}$ are fabricated and characterized by the electrochemical impedance spectroscopy (EIS). **Figure 2c** and **2d** display the C_A and phase angle (Φ) as a function of frequency, respectively. Generally, 120 Hz is a critical frequency for evaluating filtering capacitors. At this frequency, SVGAs yields a C_A of 1.72 mF cm^{-2} , which is nearly 19 times higher than that of QVGAs ($92 \mu\text{F}\cdot\text{cm}^{-2}$). More than that, the Φ_{120} of -80.6° for SVGAs is also closer to -90° compared with that of -77° for QVGAs, demonstrating the outstanding capacitive behavior of SVGAs.

COMMUNICATION

An appropriate electrode material for a high-frequency filtering capacitor should exhibit a large surface area for charge accumulation and smooth ionic transport paths to minimize the resistance. As proven by the methylene blue adsorption experiment, the SVGAs exhibit a much larger SSA than that of QVGAs (Figure S8), which explains the higher C_A of EC-SVGAs. Besides, the outstanding capacitive behavior of EC-SVGAs could be ascribed to small equivalent series resistance (ESR), which could be read out from the Nyquist plots (Figure S9). On this basis, we can conclude the strictly vertical structure and ordered graphene sheets of SVGAs maximize the utilization of surface area and provide the open channels for the shortest straight path of ions, which is in favor of excellent electrochemical performances (Figure 2f). In contrast, the agglomerated structure of QVGAs would waste the available charge adsorption surface and restrict the smooth ions transport, further increasing the distance for ion exchange (Figure 2e).

Electrochemical performances of EC-SVGAs

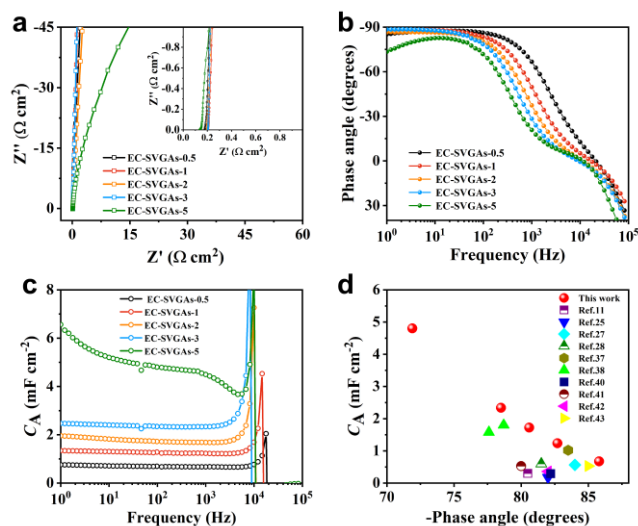


Figure 3. Electrochemical properties of SVGAs based ECs with different height. **a** Nyquist plot of EC-SVGAs with different height; inset: the expanded view at high frequencies. **b, c** Plots of Φ and C_A versus frequency for EC-SVGAs with different height. **d** Comparison of Φ and C_A of EC-SVGAs with those of reported carbon related ECs for AC line-filtering.

In addition to the vertical orientation, the height of vertical arrays prepared by EF-PECVD could be easily adjusted (Figure S10). When the electric field force is set at 30 V cm^{-1} , the height of the SVGAs increased linearly with the growth time with an average rate of $\sim 3 \mu\text{m h}^{-1}$, from $\sim 1.5 \mu\text{m}$ in half hour to $\sim 15.0 \mu\text{m}$ in 5 hours. For clarity, the different SVGAs were nominated as SVGAs- n ($n = 0.5, 1, 2, 3, 5$), where n represents the growth time. As shown in Nyquist plots (Figure 3a), all the curves exhibit the near-vertical characteristic and miss the semicircle at the high-frequency region, implying the electrochemical process is a double electric layer mechanism rather than faradic charge transfer reaction. In addition, the small relaxation time constant demonstrates the fast ion adsorption/desorption characteristic. (Figure S11) The lowest Φ_{120} of EC-SVGAs- n is measured as high as -85.8° , which is even better than commercial AECs ($22 \mu\text{F}$) (Figure S12). With the increase of height from $1.5 \mu\text{m}$ to $15.0 \mu\text{m}$, the Φ_{120} slightly

decrease in the sequence of -85.8° , -82.7° , -80.6° , -78.5° , and -71.9° (Figure 3b). Different from Φ , the C_A exhibits an incremental improvement from 0.67 to $4.80 \text{ mF}\cdot\text{cm}^{-2}$ (Figure 3c), which should be benefited from the significantly enhanced ion-accessible surface area triggered by SVGAs growth. On this basis, the area energy density (E_A) could be further calculated. (Figure S13 and Table 1) Although there are some trade-offs between the response capability and energy storage capability, the excellent C_A and E_A of EC-SVGAs- n still surpass those of the best filtering ECs based on QVGAs and most carbon-related devices reported so far (Figure 3d and Table 1).^{10, 25, 27-28, 37-38, 40-43}

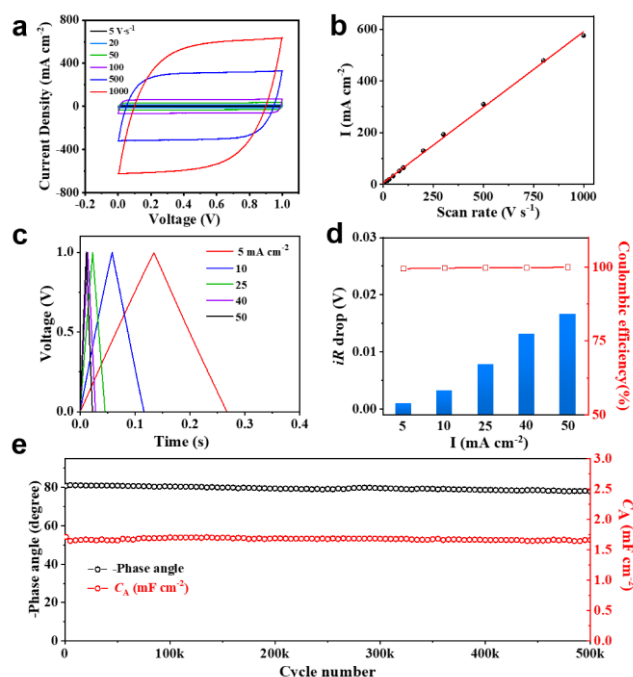


Figure 4. The electrochemical performances of EC-SVGAs-2. **a** CV curves of the EC-SVGAs-2 at scan rate up to 1000 V s^{-1} . **b** Plots of discharge current density at voltage of 0.5 V versus scan rate. **c** Galvanostatic charge-discharge curves at various current densities. **d** Voltage drop and coulombic efficiency versus current densities, respectively. **e** Cycling stability of EC-SVGAs-2.

Here, the EC-SVGAs-2 was chosen as the main object because it possesses overall best C_A of $1.72 \text{ mF}\cdot\text{cm}^{-2}$ and Φ of -80.6° at 120 Hz . As shown in Figure 4a and 4b, the cyclic voltammetry CV profiles of the EC-SVGAs-2 exhibit near rectangular shapes and linear relationship of discharge current to scan rate to $1000 \text{ V}\cdot\text{s}^{-1}$, which demonstrated fast electron transport within the electrode materials. Besides, the galvanostatic charge-discharge (GCD) measurement also confirms the impressive rate capability (Figure 4c, 4d and Figure S14). With the current density up to $50 \text{ mA}\cdot\text{cm}^{-2}$, the EC-SVGAs-2 still shows an ideal isosceles triangular shape with negligible voltage drop (iR drop), indicating the 100% coulombic efficiency and ultra-low resistance at rapid charging and discharging process. Otherwise, the intrinsic carbonaceous structure of the SVGAs endows the long-term cycling stability along with nearly unchanged C_A and Φ after striking 500 000 cycles (Figure 4e). It is worth mentioning that the EC-SVGAs also exhibit excellent flexibility, mechanical properties, and outstanding durability. (Figure S15)

COMMUNICATION

Considering the possible limitation of aqueous electrolyte (1 V), organic electrolyte and tandem configuration were eagerly extended the operation voltage to 2.5 V or X V (X means numbers of series devices) without sacrificing rectangular CV profiles (**Figure S16** and **S17**). Meanwhile, the almost coincident Bode phase diagrams between the high voltage devices and the aqueous EC-SVGAs-2 also indicate their similar capacitive behavior at a wide frequency range (**Figure S18**). Apart from the high-frequency response, the high-capacity characteristic was also retained by utilizing organic electrolyte, which delivers a C_A of $1.52 \text{ mF}\cdot\text{cm}^{-2}$ comparable to that of EC-SVGAs-2 in aqueous electrolyte ($1.72 \text{ mF}\cdot\text{cm}^{-2}$) at 120 Hz (**Figure S19**). Combining the 2.5 V working voltage, an ultra-high energy density of $0.33 \mu\text{Wh}\cdot\text{cm}^{-2}$ at $\Phi_{120} = 80.1^\circ$ can be achieved, demonstrating a significant energy storage advantage within a compact space (**Figure S13** and **Table 1**).

Filtering performance of EC-SVGAs

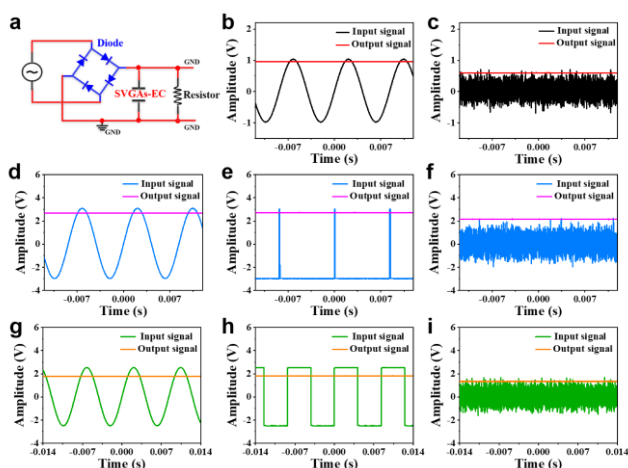


Figure 5. The filtering performances of EC-SVGAs-2. **a** Schematic demonstration of the circuit used for smoothing AC signals. **b, c** Filtering performance of EC-SVGAs unit in aqueous electrolyte. **d-f** Filtering performance of EC-SVGAs connected in series in aqueous electrolyte, **g-i** Filtering performance of EC-SVGAs unit in organic electrolyte.

Given the ultra-high frequency response and large capacity density, which are urgently required for the AC filtering performances with smooth output voltage, the EC-SVGAs was further engineered into the model AC/DC conversion circuit. **Figure 5a** displays the model circuit composed of a full-bridge rectifier, a filtering capacitor (EC-SVGAs), and a loaded resistor (R_L) connected in parallel. As a proof of concept, a series of EC-SVGAs devices with aqueous electrolyte (1 V/0.22 mF), organic electrolyte (2.5 V/0.19 mF), and tandem configuration was incorporated with $1 \text{ M}\Omega R_L$ to verify the AC filtering performances. **Figure 5b, d, e, g, h** and **Figure S20** present whether in the aqueous electrolyte or organic electrolyte, the EC-SVGAs can flat the randomly complex AC (60 Hz) to steady DC with inconsiderable ripple voltage, including the sinusoidal square, triangular, and pulse waves. More importantly, even for noise signals with sharply chaotic oscillations, the EC-SVGAs can complete the ripple filtering mission (**Figure 5c, f and i**), suggesting the EC-SVGAs have a great potential in pulse

environmental energy harvesting equipment requiring specific devices with significant filtering function.

Conclusion

This study accurately controlled the growth orientation of graphene arrays recurring to the electric-field regulated PECVD process. Compared with the previous QVGAs, the completely vertical configuration of SVGAs not only ensures straightforward pore structure from the up to down to $30 \mu\text{m}$ height, but also tremendously enhanced SSA of the materials, thus lead to efficient ion transport and electron transport pathways, and sizeable ion-accessible surface area for the high-frequency charge storage. Accordingly, the EC-SVGAs with aqueous or organic electrolyte is capable of exhibiting excellent C_A , Φ , and energy density at 120 Hz with arbitrary AC filtering performances, which is far better than most ECs based on QVGAs and carbon-related devices, demonstrating the colossal promising of EC-SVGAs for replacement of conventional AECs of practical importance.

Acknowledgements

The authors thank Yangyong Sun from Peking University, Wei Qiao from Beijing Graphene Institute for their kind suggestion and discussion on practical experiment. This work was financially supported by the Ministry of Science and Technology of China (2016YFA0200100 and 2018YFA0703502), the National Natural Science Foundation of China (Grant Nos. 52021006, 51720105003, 21790052, 21974004), the Strategic Priority Research Program of CAS (XDB36030100), and the Beijing National Laboratory for Molecular Sciences (BNLMS-CXTD-202001). This work was also supported by the Open Fund of the Key Lab of Organic Optoelectronics & Molecular Engineering.

Keywords: electric field • strictly vertical graphene arrays • specific areal capacitance • phase angle • filtering capacitor

- [1] D. P. Dubal, N. R. Chodankar, D. H. Kim, P. G. Romero, *Chem. Soc. Rev.* **2018**, *47*, 2065-2129.
- [2] M. F. El-Kady, V. Strong, S. Dubin, R. B. Kaner, *Science* **2012**, *335*, 1326-1330.
- [3] X. W. Yang, C. Cheng, Y. F. Wang, L. Qiu, D. Li, *Science* **2013**, *341*, 534-1330.
- [4] N. A. Kyeremateng, T. Brousse, D. Pech, *Nat. Nanotech.* **2017**, *12*, 7-15.
- [5] M. F. El-Kady, R. B. Kaner, *Nat. Commun.* **2013**, *4*, 1475.
- [6] E. Kim, B. J. Lee, K. Maleski, Y. Chae, Y. Lee, Y. Gogotsi, C. W. Ahn, *Nano Energy* **2021**, *81*, 105616.
- [7] M. M. Wu, F. Y. Chi, H. Y. Geng, H. Y. Ma, M. Zhang, T. T. Gao, C. Li, L. T. Qu, *Nat. Commun.* **2019**, *10*, 2855.
- [8] G. S. Gund, J. H. Park, R. Harpalsinh, M. Kota, J. H. Shin, T.-i. Kim, Y. Gogotsi, H. S. Park, *Joule* **2019**, *3*, 164-176.
- [9] N. Kurra, M. K. Hota, H. N. Alshareef, *Nano Energy* **2015**, *13*, 500-508.
- [10] F. Chi, C. Li, Q. Zhou, M. Zhang, J. Chen, X. Yu, G. Shi, *Adv. Energy Mater.* **2017**, *7*, 1700591.
- [11] Z. Fan, N. Islam, S. B. Bayne, *Nano Energy* **2017**, *39*, 306-320.

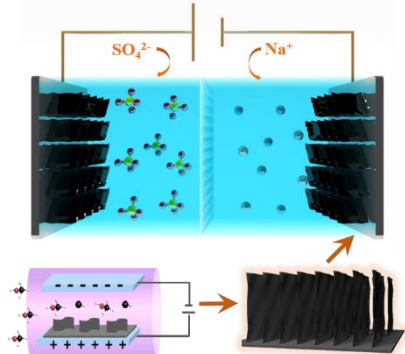
COMMUNICATION

- [12] D. Zhao, W. Chang, C. Lu, C. Yang, K. Jiang, X. Chang, H. Lin, F. Zhang, S. Han, Z. Hou, X. Zhuang, *Small* **2019**, *15*, e1901494.
- [13] D. Zhao, K. Jiang, J. Li, X. Zhu, C. Ke, S. Han, E. Kymakis, X. Zhuang, *BMC Materials* **2020**, *2*.
- [14] J. Park, W. Kim, *Adv. Energy. Mater.* **2021**, *11*, 2003306.
- [15] M. D. Stoller, R. S. Ruoff, *Energy Environ. Sci.* **2010**, *3*, 1294-1301.
- [16] M. Zhang, Q. Zhou, J. Chen, X. Yu, L. Huang, Y. Li, C. Li, G. Shi, *Energy Environ. Sci.* **2016**, *9*, 2005-2010.
- [17] Z. S. Wu, K. Parvez, X. Feng, K. Mullen, *Nat. Commun.* **2013**, *4*, 2487.
- [18] K. U. Laszczyk, K. Kobashi, S. Sakurai, A. Sekiguchi, D. N. Futaba, T. Yamada, K. Hata, *Adv. Energy. Mater.* **2015**, *5*, 1500741.
- [19] Z. Bo, M. Su, H. Yang, S. Yang, J. Yan, K. Cen, *Rev Sci Instrum* **2020**, *91*, 076105.
- [20] Z. Bo, C. Xu, H. Yang, H. Shi, J. Yan, K. Cen, K. Ostrikov, *Chem. Electro. Chem.* **2019**, *6*, 2167-2173.
- [21] S. Zheng, Z. Li, Z. S. Wu, Y. Dong, F. Zhou, S. Wang, Q. Fu, C. Sun, L. Guo, X. Bao, *ACS Nano* **2017**, *11*, 4009-4016.
- [22] C. Yang, K. S. Schellhammer, F. Ortmann, S. Sun, R. Dong, M. Karakus, Z. Mics, M. Lçffler, F. Zhang, X. D. Zhuang, E. Canovas, G. Cuniberti, M. Bonn, X. L. Feng, *Angew. Chem.* **2017**, *129*, 3978–3982.
- [23] Z. Zhang, M. Liu, X. Tian, P. Xu, C. Fu, S. Wang, Y. Liu, *Nano Energy* **2018**, *50*, 182-191.
- [24] A. Vlad, A. Balducci, *Nat. Mater.* **2017**, *16*, 161-162.
- [25] J. R. Miller, R. A. Outlaw, B. C. Holloway, *Science* **2010**, *329*, 1637-1639.
- [26] D. Pech, M. Brunet, H. Durou, P. Huang, V. Mochalin, Y. Gogotsi, P. L. Taberna, P. Simon, *Nat. Nanotech.* **2010**, *5*, 651-654.
- [27] K. Sheng, Y. Sun, C. Li, W. Yuan, G. Shi, *Sci. Rep.* **2012**, *2*, 247.
- [28] J. Lin, C. Zhang, Z. Yan, Y. Zhu, Z. Peng, R. H. Hauge, D. Natelson, J. M. Tour, *Nano Lett.* **2013**, *13*, 72-78.
- [29] Z. S. Wu, Z. Liu, K. Parvez, X. Feng, K. Mullen, *Adv. Mater.* **2015**, *27*, 3669-3675.
- [30] Y. Rangom, X. W. Tang, L. F. Nazar, *ACS Nano* **2015**, *9*, 7248-7255.
- [31] S. T. Senthikumar, Y. Wang, H. Huang, *J. Mater. Chem. A* **2015**, *3*, 20863-20879.
- [32] K. Gao, S. Wang, W. Liu, Y. Yue, J. Rao, J. Su, L. Li, Z. Zhang, N. Liu, L. Xiong, Y. Gao, *Chem. Electro. Chem.* **2019**, *6*, 1450-1457.
- [33] Q. Zhou, M. Zhang, J. Chen, J. D. Hong, G. Shi, *ACS Appl. Mater. Inter.* **2016**, *8*, 20741-20747.
- [34] Y. Xu, Z. Lin, X. Zhong, X. Huang, N. O. Weiss, Y. Huang, X. Duan, *Nat. Commun.* **2014**, *5*, 4554.
- [35] N. Islam, S. Li, G. Ren, Y. Zu, J. Warzywoda, S. Wang, Z. Fan, *Nano Energy* **2017**, *40*, 107-114.
- [36] J. R. Miller, R. A. Outlaw, *J. Electrochem. Soc.* **2015**, *162*, 5077-5082.
- [37] M. Zhang, W. Wang, L. Tan, M. Eriksson, M. Wu, H. Ma, H. Wang, L. Qu, J. Yuan, *Energy Storage Mater.* **2021**, *35*, 327-333.
- [38] J. Park, J. Lee, W. Kim, *ACS Energy Lett.* **2021**, *6*, 769.
- [39] H. Zhang, D. Yang, A. Lau, T. Ma, H. Lin, B. Jia, *Small* **2021**, *17*, e2007311.
- [40] C. Zhang, H. Du, K. Ma, Z. Yuan, *Adv. Energy. Mater.* **2020**, *10*, 2002132.
- [41] G. Ren, S. Li, Z. X. Fan, M. N. F. Hoque, Z. Fan, *J. Power Sources* **2016**, *325*, 152-160.
- [42] G. Ren, X. Pan, S. Bayne, Z. Fan, *Carbon* **2014**, *71*, 94-101.
- [43] M. Z. Cai, R. A. Outlaw, R. A. Quinlan, D. Premathilake, S. M. Butler, J. R. Miller, *ACS Nano* **2014**, *8*, 5873-5882.
- [44] M. Cai, R. A. Outlaw, S. M. Butler, J. R. Miller, *Carbon* **2012**, *50*, 5481-5488.
- [45] D. Premathilake, R. A. Outlaw, R. A. Quinlan, S. G. Parler, S. M. Butler, J. R. Miller, *J. Electrochem. Soc.* **2018**, *165*, 924-931.
- [46] M. Zhu, J. Wang, B. C. Holloway, R. A. Outlaw, X. Zhao, K. Hou, V. Shutthanandan, D. M. Manos, *Carbon* **2007**, *45*, 2229-2234.
- [47] Z. Bo, Y. Yang, J. Chen, K. Yu, J. Yan, K. Cen, *Nanoscale* **2013**, *5*, 5180-5204.
- [48] S. Xu, J. Zhang, *Small Structures* **2020**, *1*, 2000034.
- [49] J. R. Miller, R. A. Outlaw, B. C. Holloway, *Electrochimica Acta* **2011**, *56*, 10443-10449.
- [50] S. Xu, S. Wang, Z. Chen, Y. Sun, Z. Gao, H. Zhang, J. Zhang, *Adv. Funct. Mater.* **2020**, *30*, 2003302.
- [51] Y. G. Zhang, A. Chang, J. Cao, Q. Wang, W. Kim, Y. M. Li, N. Morris, z E. Yenlime, J. Kong, H. J. Dai, *Appl. Phys. Lett.* **2001**, *78*, 3155-3157.

COMMUNICATION

Entry for the Table of Contents

Insert graphic for Table of Contents here.



An electric-field assisted PECVD method was developed to grow strictly vertical graphene arrays (SVGAs) as electrode materials of ECs. Accordingly, the EC-SVGAs with aqueous or organic electrolyte is capable of exhibiting excellent C_A of $1.72 \text{ mF}\cdot\text{cm}^{-2}$, Φ of 80.6° , and energy density of $0.33 \mu\text{Wh}\cdot\text{cm}^{-2}$ at 120 Hz with arbitrary AC filtering performances, which is far better than most carbon-related devices, demonstrating the colossal promising for replacement of conventional AECs.